Journal of Advanced Concrete Technology Vol. 17, 715-727, December 2019 / Copyright © 2019 Japan Concrete Institute 

*Scientific paper*

# Fatigue Lifetime Prediction of Newly Constructed RC Road Bridge Decks

Eissa Fathalla[1], Yasushi Tanaka[2*] and Koichi Maekawa[3]

Received 17 July 2019, accepted 13 December 2019 doi:10.3151/jact.17.715


## Abstract

Multiple factors, regarding mechanical properties, load levels, and environmental conditions, affect the fatigue lifetime of reinforced concrete (RC) bridge decks. For the mechanical behavior, previous research predicts the fatigue lifetime of RC decks as a function of their punching shear capacity, where they give less attention to other modes of failure due to experimental limitations of fatigue loading and the restriction of girders spacing in the past design practice. Nowadays, multi-scale simulation can deal with fatigue loading problems, which secures examining complex situations that cannot be easily reproduced in the laboratories of fatigue tests. In this study, various RC decks with wide range of dimensions, material properties, reinforcement ratio, and load levels are analyzed by the validated multi-scale simulation. Then, artificial neural network (ANN) based model is also proposed based on wide-range of studied cases, which estimates the fatigue life of newly constructed RC decks, where it can be the basis of performance-based design. After that, the impact of deck's properties on fatigue life is evaluated based on the built ANN model, which matches the conceptual design of RC decks. Finally, coupling of an empirical equation and ANN model is proposed, which may support conceptual decision-making.


## 1. Introduction

Lifetime of reinforced concrete (RC) bridge decks are governed by multiple factors from mechanical and environmental points of view. The global life of RC decks is subjected to the mechanical fatigue-behavior (Lee and Barr 2004; Maekawa et al. 2006a; Matsui 2007; Matsui and Maeda 1986; Schläfli and Brühwiler 1998; Sparks and Menzies 1973; Tepfers and Kutti 1979), while site-inspected damage from environmental conditions is the local factor, which can reduce this global life. In other words, the remaining life of RC decks can be simply estimated as the multiplication of the global life from mechanical properties and the deterioration rank of site-inspected damage from environmental conditions.

It was reported that RC decks experience performance-degradation due to environmental attacks such as corrosion, alkali silica reaction, freeze and thawing, stagnant water, and site-inspected cracking (Freyermuth *et al.* 1970; Cady and Weyers 1983; Maeshima *et al.* 2014; Val *et al.* 1998; Vassie 1984; Lindquist *et al.* 2006; Ulm *et al.* 2000; Sakulich and Bentz 2011; Detwiler *et al.* 1997; Maekawa and Fujiyama 2013a, 2013b; Matsui 1987; Waagaard 1982; Shah *et al.* 1998; Tanaka *et al.* 2017; Ohta *et al.* 2015). In previous research, the deterioration ranks of site-inspected cracks on bottom surface and stagnant wetting locations were strictly obtained to achieve the reduction in life of RC decks compared to their sound condition with no damage (Fathalla *et al.* 2018a, 2018b, 2019a, 2019b, 2019c).

In the past few decades, performance-based design was introduced in the structural field in order to overcome the drawbacks of ordinary regulations and design codes (Walraven 2013; CSA 2014). Traditional codes were built mainly on the ultimate design methods and/or working-stress design methods. They were not directly based on structure's performances but were deemed to satisfy the design requirements. Development of new types of structures and technologies were requested to indicate the performance required in design. Thus, the performance-based design has been introduced to fill the gap between the prescriptive process and structure's performance in reality. The concept of performance-based design agrees with the era of maintenance. Repair, strengthening and the renewal design should be performance-based to achieve reliability.

Experimental studies introduced the fatigue lifetime-estimation of RC decks in sound conditions based upon their static shear strength (Matsui 2007). Most of these studies purely focused on a mode of failure like punching shear failure. In fact, fatigue experiments are usually conducted with constant dimensions of slabs and supporting conditions due to the huge time and running cost of tests. Thus, complex fatigue behavior of slabs with various dimensions was not fully completed experimentally.

Nowadays, multi-scale simulation can deal with fatigue loading problems of wide validation (Maekawa *et*


[1]Lecturer, Structural Engineering Department, Cairo University, Giza 12613, Egypt.
[2]Associate Professor, Kanazawa Institute of Technology, 7-1, Ohgigaoka, Nonoichi, Ishikawa, Japan.
*Corresponding author,
*E-mail*: ytanaka@neptune.kanazawa-it.ac.jp
[3]Professor, Yokohama National University, 79-1, Tokiwadai, Hodogaya, Yokohama, Japan.

*al.* 2003, 2009, 2006a, 2015). The constitutive laws for high cycle tension, compression, and shear transfer were upgraded during the past decades, where each constitutive law was brought into complex-stress paths. The fatigue lifetime simulation is based on direct path integral scheme (Maekawa *et al.* 2006a). Thus, it may estimate the fatigue capacity in such a case of convoluted-stress paths like travelling-wheel loading.

First, in this research, the deck's properties that are thought to have minimal impact on fatigue life are checked by the multi-scale simulation. The role of this study is to eliminate the unnecessary deck's information for building the predictive method for RC fatigue life in sound conditions. On the basis of findings of effective variables of deck's properties, many RC decks with wide ranges of properties, dimensions, material properties, reinforcement, and load levels are analyzed by the lifetime simulation, which are used for building the fatigue capacity as a compilation of all influencing factors.

Although multi scale simulation enables to estimate the fatigue life of RC deck with any kinds of properties, currently, it still needs a significant computational time including pre-post processing. This is a burden to seek for the dimensioning of slabs through the try-and-error search in design process of newly constructed bridges. Then, artificial neural network (ANN) is introduced as the second step on the basis of the simulation results, which secure to obtain the fatigue life of newly constructed RC decks. Bayesian regularization technique is utilized for training in order to reduce the risk of overfitting problem. The generalization of the proposed ANN model is secured by conducting leave-one-out cross-validation and testing among unknown data. Nowadays, ANN model is easy to be used owing to the distributed frameworks. It is difficult to understand how it thinks because ANN model is just a set of weights' matrices.

To interpret ANN model, the impact of ANN's input variables, which are the deck's properties, on the fatigue life of RC decks is evaluated based upon the built ANN model as third step. These results are discussed in terms of the conceptual design of RC decks. Finally, an empirical equation that aims to guide the effective design of RC deck with the use of ANN model is tried and checked by analyzing RC decks from sites in Japan.

## 2. Methodology

### 2.1 Multi-scale simulation

For fatigue loading simulation, the multi-scale simulation program is used, which has been experimentally validated (Maekawa *et al.* 2003, 2009, 2006a, 2015). **Figure 1** shows the set of constitutive laws of the cracked concrete for high-cycle path and time-dependent constitutive models (Maekawa *et al.* 2006a). These constitutive laws indicate the damage caused by high cycle stress paths with regard to degrading stiffness and progressive plasticity in tension, compression and shear along cracks. The multi-scale analysis can estimate the members' capacity on the convoluted stress paths like the moving wheel-type loads based upon the direct-path integral scheme (Maekawa *et al.* 2006a).

The concrete's damage due to fatigue is taken into consideration in compression and tension, where the elastic stiffness of concrete rooted in the micro-cracks

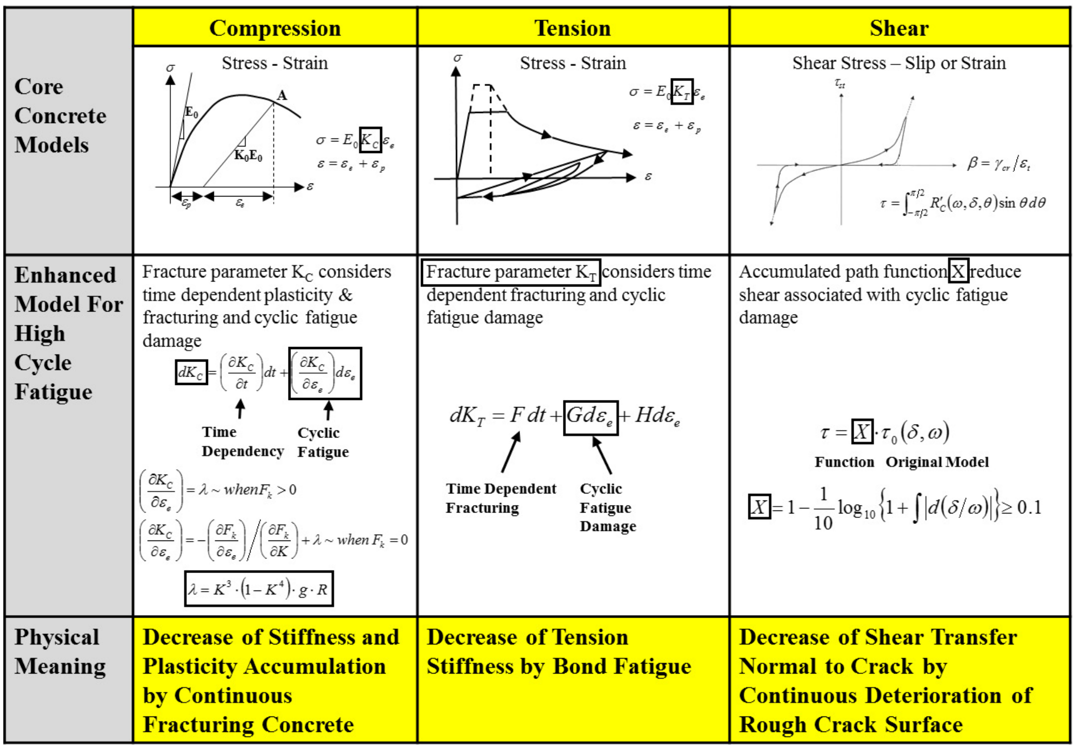

Fig. 1 Constitutive laws for high-cycle fatigue of reinforced concrete.

reduces gradually during the fatigue loading. This fatigue damage mechanism is expressed by the evolution law of the damage parameter ($K_C$) that indicates strain rate's effect and we have,

$$\varepsilon = \varepsilon_e + \varepsilon_p \tag{1}$$

$$\sigma = E_o \varepsilon_e K_c \tag{2}$$

$$dK_c = \left(\frac{\partial K_c}{\partial t}\right) dt + \left(\frac{\partial K_c}{\partial \varepsilon_e}\right) d\varepsilon_e \tag{3}$$

$$d\varepsilon_p = \left(\frac{\partial \varepsilon_p}{\partial t}\right) dt + \left(\frac{\partial \varepsilon_p}{\partial \varepsilon_e}\right) d\varepsilon_e \tag{4}$$

where, $\varepsilon$ is the total strain, $\varepsilon_e$ is the elastic strain, $\varepsilon_p$ is the plastic strain, $\sigma$ is the total stress, $E_o$ is the initial stiffness, and $K_c$ is the damaging parameter (damage evolution due to internal stresses' repetitions is implemented in the rate type evolution of $K_c$).

The reduced stiffness owing to the bond fatigue of concrete and reinforcement is expressed by ($K_T$) in the scheme of tension stiffening concept. Thus, we have,

$$\sigma = E_o \varepsilon K_T \tag{5}$$

$$dK_T = Fdt + Gd\varepsilon + Hd\varepsilon \tag{6}$$

where, F indicates time dependent fracturing as tension creep, H indicates instantaneous fracture, and G indicates the fracture damage induced by high cycle load repetitions, considering the loss of bond between reinforcement and concrete.

The crack planes show roughness rooted in the size of suspended aggregates. This roughness is gradually smoothened under cyclic effects of shear slip until the aggregates-interlock is gradually lost. This damage is considered by adding the term (X) to the formulation in order to decrease the shear transfer according to the number of cycles, as indicated by Equations 7-8.

$$\tau = (X).\ \tau_{or.}(\delta, \omega) \tag{7}$$

$$X = 1 - \frac{1}{10}\log_{10}(1 + \int |\, d(\frac{\delta}{\omega})\,|) \tag{8}$$

where, $\tau$ is transferred shear under high cycle load, $\tau_{or}$ is the transferred shear stress calculated by the referential contact density function (Li and Maekawa 1988), $\omega$ is the crack width, $\delta$ is the crack slip, and X is the fatigue modification factor considering accumulation of shear deformation during the loading cycles.

The multi-scale simulation can successfully capture various modes of failure, i.e., out-of-plane shear, punching shear and tied-arch mechanism. It had been validated with experimental setups under different types of fatigue loading applied to deck specimens in previous research (Maekawa *et al.* 2006b) as shown in **Fig. 2**.

## 2.2 Artificial neural network

Artificial neural network (ANN) is a powerful method for building predictive models of complex problems with high non-linearity, where it is inspired from biological nervous system (Fausett 1994; M. I. T-Lincoln Laboratory 1989; Grossberg 1982; Hagan *et al.* 1996). In previous studies (Fathalla *et al.* 2018, 2019a), ANN

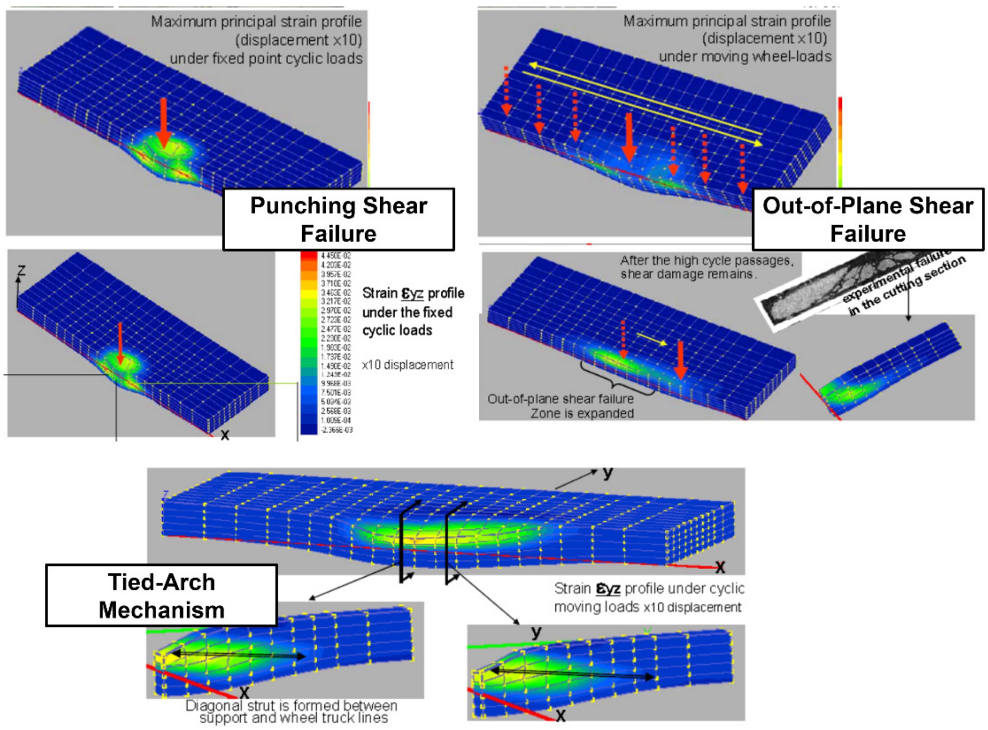


Fig. 2 Examples of failure modes of RC decks captured by multi-scale simulation (Maekawa *et al.* 2006b).

models were introduced for remaining fatigue life assessment of RC decks based upon site-inspected cracks of dry and submerged water states. ANN's input was cracks' location and width, while the ANN's output is the remaining fatigue life. These ANN models offer the deterioration rank in just seconds by shooting the bottom surface of RC decks with a high-resolution camera, as shown in **Fig. 3**. Thus, reliable maintenance plan could be conducted based on rational assessment of deteriorated RC decks. Moreover, on the basis of the weights assigned with the synapses of the built ANN models with single neuron, hazard maps for the location of higher hazardous cracking were obtained (see **Fig. 3**), where physico-mechanistic expressions were found. Thus, these hazard maps satisfy the site-inspectors needs.

## 3. Finite element (FE) analysis of wheel load on RC decks

### 3.1 RC deck

The targeted problem of this paper is RC decks of steel-girder road bridges. They are supported by main girders in the longitudinal direction of the bridge, where main girders are connected by cross beams in the transverse direction in order to secure their lateral stability. **Figure 4** shows the design properties of RC decks, which includes compressive strength, reinforcement rebar, span-width, thickness, concrete cover, and design wheel load. It should be noted that, in fact, RC decks are conservatively designed as one-way slab, where the traffic loads are mainly transmitted to the longitudinal girders.

### 3.2 Loading scheme and boundary conditions

The simulation model of the studied RC decks is discretized in the x-y plane to mesh size of (250 × 250 mm), while it is discretized into four layers in the z-direction, as shown in **Fig. 4**. The length of the RC decks depends on several factors such as bridge type, however in a previous research (Fathalla *et al.* 2018a), 6.0-meters length was found to be optimum as a reference of existing slabs in service.

The speed of the travelling load is selected as 60 km/h, which is the legal speed limit for Japan's national routes. The dimensions of the wheel load are 500 and 250 mm corresponding to the contact area of vehicle tires (see **Fig. 4)**. The boundary conditions are chosen to be hinged supports, which allow rotational motion and restraint the translational motion. In reality, some rotational restrains exist since the RC decks are generally connected to the top flanges of longitudinal steel girders by studs and/or bolts. In addition, the torsional rigidity of the steel girders also affects the degree of rotational restraint at the deck's boundaries. Here, the selected boundary conditions are on the conservative side for estimating the fatigue life of RC decks.

### 3.3 Failure criterion

According to past fatigue-experimental programs, the fatigue limit state was based upon the central live load deflection (Tanaka *et al*. 2017; Maeshima *et al*. 2014). When its deflection (Equation 9) reaches (2.5~3.5) times of its initial value, the deck is judged to fail in fatigue. This limit state (Equation 10) corresponds to the one of bond-loss between main reinforcement and concrete.

Generally, this fatigue failure criterion was found to be reasonable since the deck's properties are explicitly included in the mere values of live load deflection. In addition, in most cases, shear failure of concrete occurs before the fatigue rupture of reinforcement (Matsui *et al.* 1986). Thus, this criterion is expected to be rational for fatigue life estimation of RC decks. It should be noted that this failure criterion targets the serviceability limit

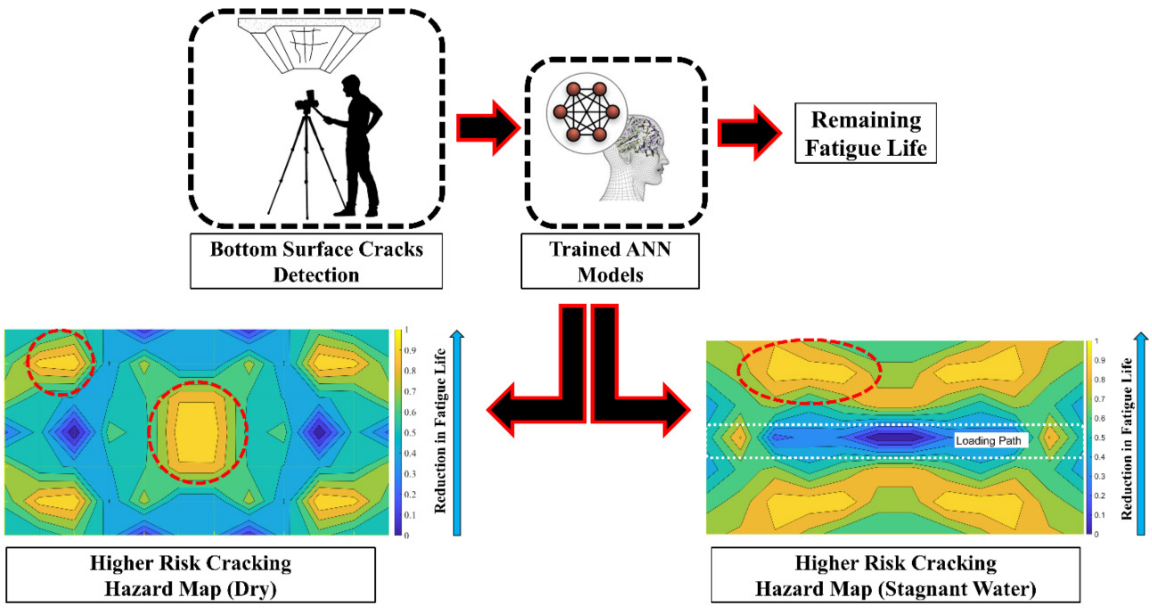


Fig. 3 Predictive models and hazard maps based on ANN (Fathalla *et al.* 2018, 2019a).

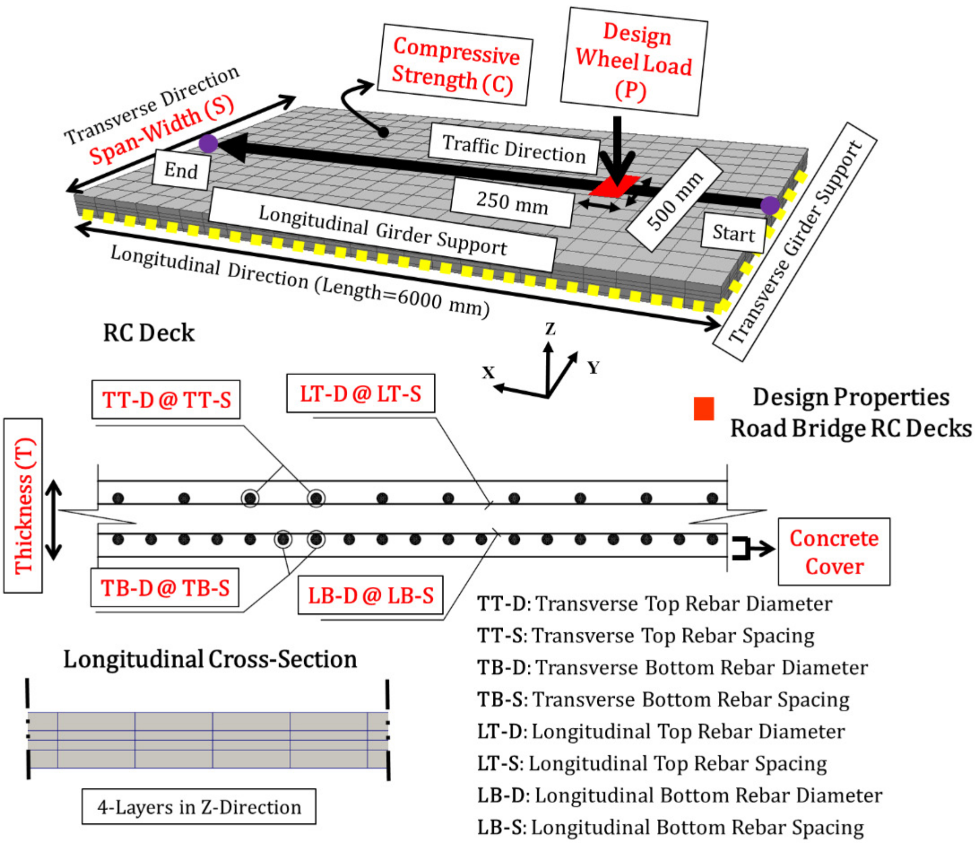


Fig. 4 Design properties of RC decks of road steel-girder bridges.

state, where the decks do not reach the total collapse even though we may estimate the load carrying mechanism. Thus, a few failure modes are fairly predicted from the load carrying mechanism as,

$$\delta_{L,N} = \delta_{1,N} - \delta_{2,N} \quad (9)$$

$$\delta_{L,N} / \delta_{L,0} \geq 3.0 \quad (10)$$

where $\delta_{L,N}$ is the central live load deflection at N cycles, $\delta_{1,N}$ is the central total deflection at N cycles at the loading stage, $\delta_{2,N}$ is the central total deflection at N cycles at the unloading stage, $\delta_{L,0}$ is the initial live load deflection, and $N_F$ is number of cycles where $\delta_{L,N}$ reaches limit stats (Equation 10).

### 3.4 Comparison of numerical results and experiment

Above mentioned FE analysis has been compared with several experiments of wheel running tests. Fujiyama *et al.* (2013) conducted fatigue analyses of wheel running experiments reported by Okada *et al.* (1982). Numerical result successfully showed the evolved deformation as the loading cycle goes ahead. Other wheel running tests with different dimensions and setups have been also examined (e.g. Hiratsuka *et al.* 2016 and Tanaka *et al.* 2017) and numerical results were validated to match the experimental facts. Multi-scale analysis was also used in the simulation of steel-concrete composite deck (Fujiyama *et al.* 2014b) and the successful result was reported. Thus, moving wheel-type load fatigue analysis with multi-scale simulation has been already examined with the past experiments. In the next step, we try to use multi-scale simulation not only to trace a single target deck but also to get responses of various ones. Then, collected data was analyzed statistically with use of ANN as discussed in the following sections.

## 4. Predictive model

### 4.1 Necessary information for building the predictive model

Mechanically, the governing factors for the fatigue life of RC decks are deck's thickness, span-width in the transverse direction, bottom reinforcement in the transverse direction, compressive strength of concrete, and load levels (Fathalla *et al.* 2018c). On the other hand, concrete cover, and other reinforcement rebar (top rebar and bottom rebar in the longitudinal direction) should logically have a minor impact on the fatigue life from a mechanical point of view. In order to check the necessity of including these factors in building the simplified model, a sensitivity analysis is conducted, where each factor is checked with wide ranges, while the rest of properties are kept the same, as shown in **Tables 1** and **2**. In this sensitivity analysis, loading wheel of 98 kN is selected, which is the design load [Japanese Specifications for Highway Bridges Part-III (JRA 2012)].

Table 1 Material Properties of the reference deck for sensitivity analysis.

| Material Type | | Concrete | Steel Reinforcement |
|---|---|---|---|
| Young's Modulus | $N/mm^2$ | 24,750 | 205,000 |
| Compressive Strength | $N/mm^2$ | 30 | 295 |
| Tensile Strength | $N/mm^2$ | 2.2 | 295 |
| Specific Weight | $kN/m^3$ | 24 | 78 |

Table 2 Dimensions and reinforcement rebar of the reference deck for sensitivity analysis.

| S (mm) | T (mm) | Concrete Cover (mm) | Reinforcement Rebar* (mm) | | | | | | | |
|---|---|---|---|---|---|---|---|---|---|---|
| | | | TT-D | TT-S | TB-D | TB-S | LT-D | LT-S | LB-D | LB-S |
| 3500 | 180 | 30 | 16 | 200 | 16 | 100 | 13 | 200 | 13 | 100 |

*Referred to in Fig. 4.

**Figure 5** shows the relation of wide range of concrete covers and their corresponding fatigue life analyzed by the multi-scale simulation. The results show that concrete cover has minor effect on fatigue life of RC decks, where the coefficient of variation (C.O.V) of the studied cases with respect to the reference one (30 mm) is around 14%. Thus, it can be neglected from a mechanical point of view.

On the other hand, **Figs. 6 - 8** show the sensitivity of wide range of reinforcement ratio for longitudinal bottom, longitudinal top, and transverse top rebar on fatigue life, respectively, where the reinforcement ratio (RFT%) is calculated from Equation 11. It is clear that the reinforcement has a less impact on remaining fatigue life, where the C.O.V of the analyzed cases with respect to the reference one is around 21%, 5%, and 9%, respectively. This can be explained from a structural point of view. Generally, RC decks are designed as a one-way slab, where the loads are mainly transmitted transversely to the longitudinal steel-girder supports. Thus, the transverse bottom rebar should be the main design reinforcement.

From the series of sensitivity analysis, we can conclude that excluding some variables (concrete cover, top rebar, and bottom rebar in the longitudinal direction) from building the predictive model is acceptable in practical point of view. Moreover, we should keep in mind that the key factor for building a simplified formula and an ANN model is to seek for the best performance input variables on the scheme of conceptual design (Fathalla *et al.* 2018a).

Table 3 Maximum and minimum range of deck's properties (ANN's dataset).

| Deck's Properties | Minimum | Maximum |
|---|---|---|
| Span-Width (mm) | 1000 | 3500 |
| Thickness (mm) | 150 | 240 |
| Compressive Strength (MPa) | 18 | 60 |
| Reinforcement Ratio % | 0.56 | 2.73 |
| Wheel Load (kN) | 90 | 300 |

$$RFT\% = A/(10 \times T) \quad (11)$$

where, A is the area of one directional layer of reinforcement rebar ($mm^2$ /m') and T is deck's thickness (mm).

### 4.2 ANN dataset

A total of 75 samples are prepared for a wide range of the width, slab thickness, transverse bottom reinforcement ratio, compressive strength, and load levels. **Table 3** shows the wide range of deck's properties of studied cases, where it covers probable cases in practice. Note that the increase of training data does not always lead to better ANN model because the number of parameters is rather small in this case. More important point is that the data from multi-scale simulation should cover various cases as much as possible.

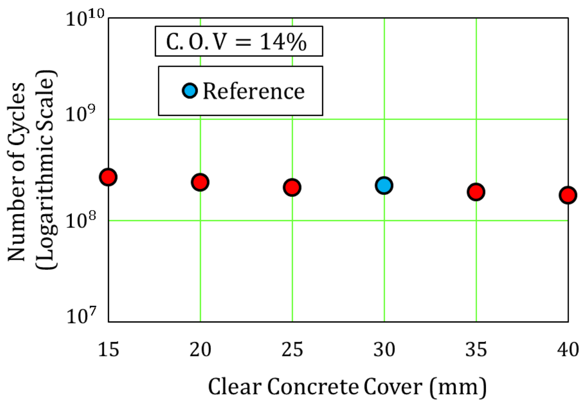


Fig. 5 Relation of the concrete cover and the fatigue life of RC decks.

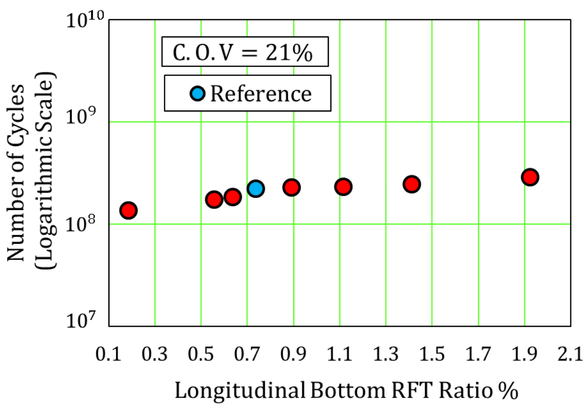


Fig. 6 Relation of the longitudinal bottom reinforcement ratio and the fatigue life of RC decks.

### 4.3 Neural network platform and structure

The platform used to conduct ANN algorithm is MATLAB R2017a-Neural Networks Toolbox. Unidirectional feedforward network and Bayesian regularization training function are selected for conducting the ANN (Hagan *et al*. 1996; Murphy 2012; Hagan and Menhaj 1994; Rumelhart *et al*. 1986; Burden and Winkler 2008; Foresee and Hagan 1997; MacKay 1992). Bayesian regularization neural network (BRANN) in most cases is robust to sidestep overfitting, where it uses L2 regularization, thus, it is expected to secure generalization (MacKay 1992). The structure of the conducted ANN is one hidden layer with six neurons. It should be noted that the ANN's structure is chosen to achieve the best performance and to avoid overfitting of ANN's model, where the size of the network should be optimum.

### 4.4 Neural network input variables and output

**Table 4** shows the input variables and the output of the proposed ANN Model, where it consists of five input variables and one output value which is the fatigue life. The datasets for both training and validating ANN are created by the multi-scale simulation and they are the input of the machine-learning block as well. The training data are used to adjust the weights of the neurons of the ANN and the test dataset is used only once after the training are finished to check the validity of the training. After training with the dataset in the machine-learning block, if the ANN can correctly map the training data and identify the testing data, it is considered as a fairly built ANN. At last, the remaining fatigue life can be obtained for any RC deck in a sound condition in just a moment without running multi-scale simulation with complex procedures such as mesh generation with wheel traveling load, analysis of tens of thousands steps of numerical results and so on.

Table 4 ANN's input variables and output.

| ANN's Input Variables | ANN's Output |
|---|---|
| Span-Width (mm)<br>Thickness (mm)<br>Compressive Strength (MPa)<br>Reinforcement Ratio %<br>Wheel Load (kN) | Fatigue Life<br>(Number of Cycles) |

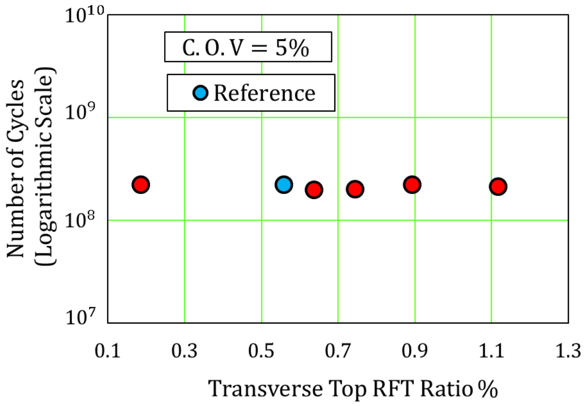


Fig. 7 Relation of the transverse top reinforcement ratio and the fatigue life of RC decks.

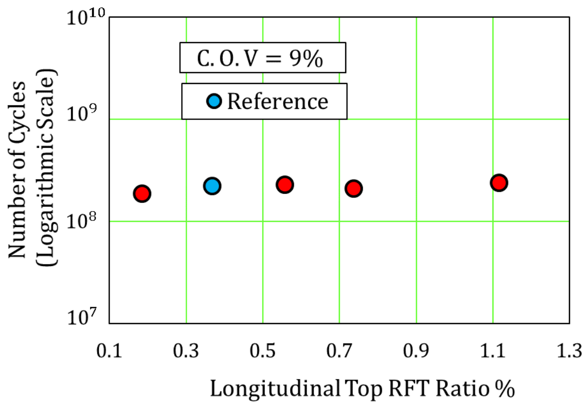


Fig. 8 Relation of the longitudinal top reinforcement ratio and the fatigue life of RC decks.

### 4.5 Leave-one-out cross-validation

In order to achieve reliable evaluation for the used training method and network's size, leave-one-out cross-validation (CV) is conducted (Geisser 1993; Picard and Cook 1984). In the cross validation (leave-one-out), the dataset (75 data) is divided into 75 subsets. Then, each division (1 data) is treated as a validation dataset and the rest of it (74 data) is treated as a training dataset. This training and validation processes are repeated against every subset. Consequently, the prediction errors of the validation subsets are statistically obtained as shown in **Fig. 9**. The coefficient of variation (C.O.V) of prediction of the cross-validation demonstrates the generalization of the prediction, where it only reaches 24%.

### 4.6 ANN model evaluation

The dataset is divided into training dataset (84%) and the test one (16%). The ratio of these datasets is empirically determined. Then, Bayesian regularization technique is used for training the ANN model. **Figure 10** shows the ANN results, where it maps the training data and identify the test data with good accuracy. The coef-

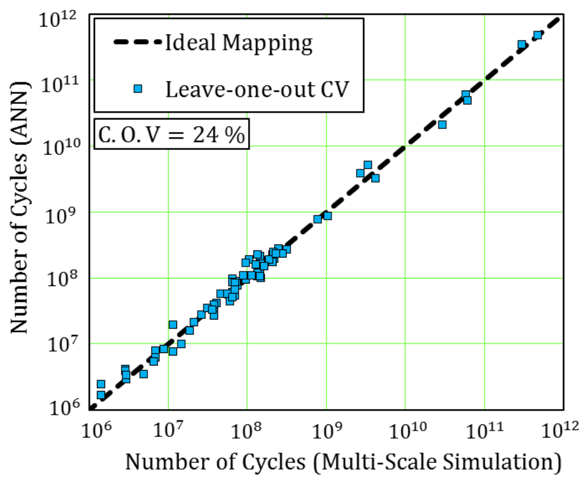


Fig. 9 Leave-one-out cross-validation results.

ficient of variation of prediction (C.O.V) for training and test data are 17% and 47%, respectively. Moreover, the network's performance is monitored during the training scheme. **Figures 11** and **12** show the evolution of the network's mean square errors and the sum of the square of weights and biases with training's epochs, respectively, where they reach stable states (best performance at 1312 epochs). Generally, in the Bayesian regularization scheme, if the network performance parameters reach stable states, it means that the network is truly converged. In this scheme, training is terminated basically if the mean square error or its slope reduces until the limit or the number of epochs reaches the predefined maximum limit. Thus, the results demonstrate the robustness of prediction of the proposed ANN model.

### 4.7 ANN's assessment of the effect of deck's properties on fatigue life

In order to evaluate the deck's properties effect on fatigue life in terms of the built ANN model, a sensitivity analysis has been performed on the basis of properties of the referential RC deck. The role of this sensitivity analysis is to visualize the way of thinking by the ANN model for us.

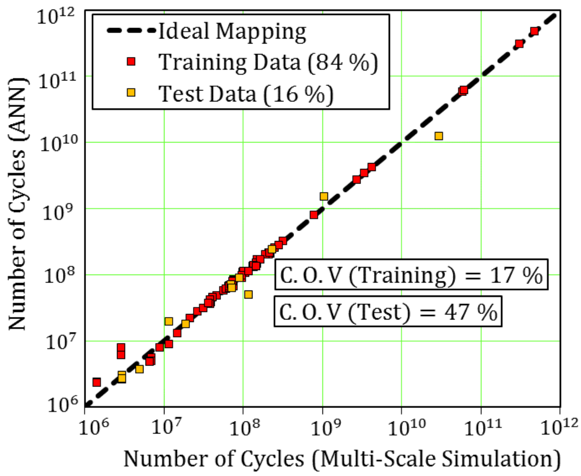


Fig. 10 ANN model prediction accuracy.

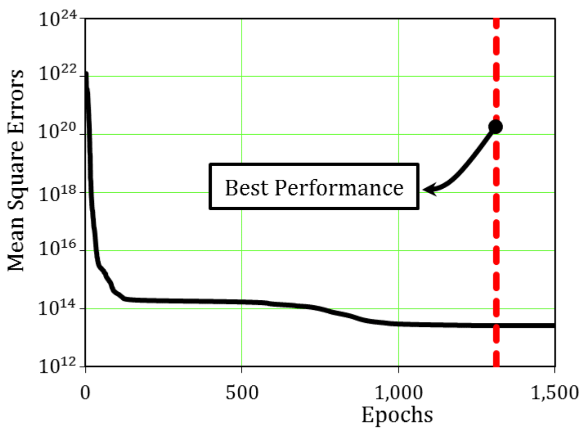


Fig. 11 Relation of network's mean square errors and training's epochs.

In this comparison, each deck's property is checked with wide ranges, while the rest of the properties are kept fixed as the referential RC deck. **Figure 13** shows the ANN's estimated fatigue lives of wide range of each property, normalized by the referential RC deck properties. It is clear that the span-width is the most effective parameter to upgrade the fatigue life, mostly when the span-width is reduced to less than 2.0 meters (span/thickness less than 12), where it can be seen from the slope of span-width's curve. This event occurs since the behavior of the RC deck at this point changes from truss action to the so-called tied-arch by the formation of struts that transmit the load directly to the boundary supports (Bakht 1996; Rankin *et al.* 1997). This phenomenon is similar to the diagonal tension failure in the case of RC beams (Fenwick and Thomas 1968; Kim *et al.* 1997; Zararis *et al.* 2001). Generally, the diagonal shear strength of RC beams is almost the same when shear span to effective depth ratio (a/d) is 2.5 or more. Contrarily, shear strength increases significantly if (a/d) is less than around 2.0.

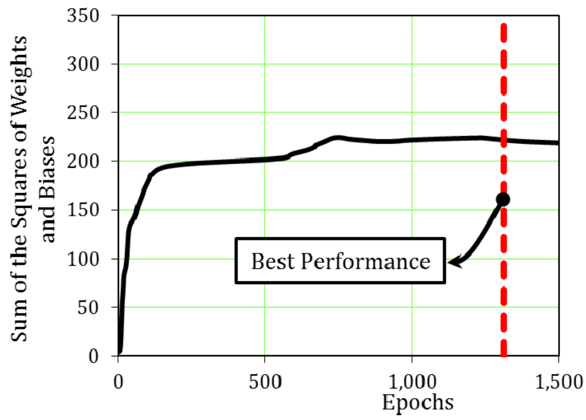


Fig. 12 Relation of network's sum of the squares of weights and biases, and training's epochs.

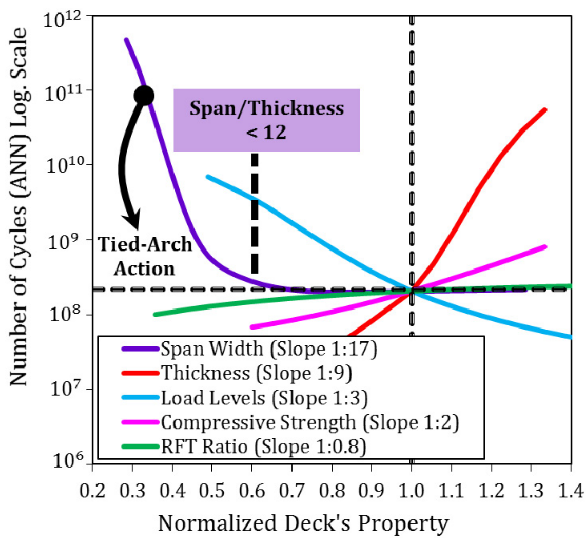


Fig. 13 Relation of normalized referential deck's property and estimated fatigue life by ANN.

The second effective parameter is found to be the deck's thickness. By increasing the deck's thickness by 5%, we can obtain an extension in life around 45% on logarithmic scale, which corresponds to 300% on actual scale. Currently in Japan, most of the RC decks are constructed with large thickness more than (240 mm) in most situations, while existing thin decks were constructed some decades ago. Thus, these results demonstrate the effectiveness of the recent design codes (JRA 2012).

The third effective parameters are the load levels and the compressive strength, where the slopes of their curves are close to each other. Finally, it is obvious that the least effective parameter is the reinforcement ratio of the transverse bottom rebar, where these results matches the conceptual design of slabs. In design specifications (JSCE 2007), the shear capacity of the slab is directly proportional to the cubic root of reinforcement ratio. Then, the reinforcement ratio has a small impact on slab's shear capacity, which matches the ANN's inferences.

It is found that the starting point of the tied-arch action is dependent on the compressive strength by comparing thin (180 mm) with thick (220 mm) decks with different compressive strength (30, 50 MPa) in consideration of widely varying span to thickness ratio, as shown in **Fig. 14.** This threshold of the span to thickness ratio increases for higher compressive strength. Moreover, this effect is found to be more significant in the case of thick decks compared to thin ones.

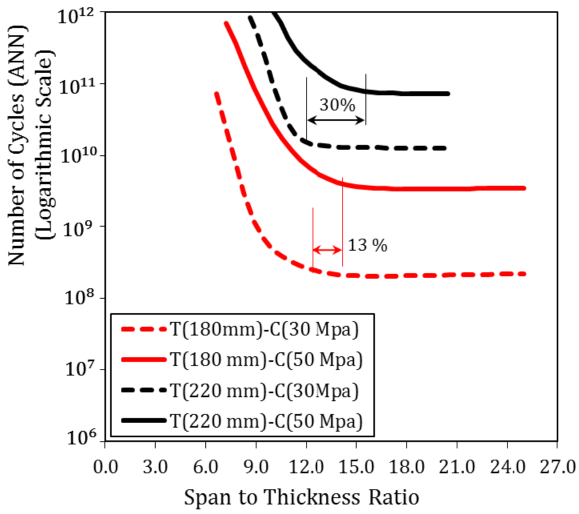

Fig. 14 Effect of compressive strength on the threshold of tied-arch action.

### 4.8 Tied-arch actions of RC decks

For further investigation of arch and truss actions, two RC decks of 16 cm thickness are analyzed with different span-width (1.0 and 3.0 meters) by the multi-scale simulation. The rest of material properties and reinforcement details are kept the same as the reference case (Section 4.1).

The progressive central maximum total load deflection with loading cycles for both cases is shown in **Fig. 15**, where the difference in their remaining fatigue life is around 56 times. **Figures 16** and **17** show the shear strain distributions among their central transverse cross-section (1.0 and 3.0 meters) at 3,000 loading cycles, respectively. For the case of small span-width (1.0 meters), the shear localization is at the zone connecting wheel-load and boundary supports, where diagonal compression occurs at this region as a phenomenon so called tied-arch action. Thus, the wheel-load is directly transferred to the supports leading to upgraded fatigue life. The results demonstrate that fatigue life of existing RC decks could be upgraded by installing stringers on site in order to reduce their span-width. For the case of wide span-width (3.0 meters), the shear localization is found to be just below the loading path, where the behavior of RC deck is governed by punching shear failure mode.

## 5. ANN model in design

### 5.1 Proposal of design process with ANN model

Although finite element (FE) simulation can solve any problem with any shape, dimension and boundary con-

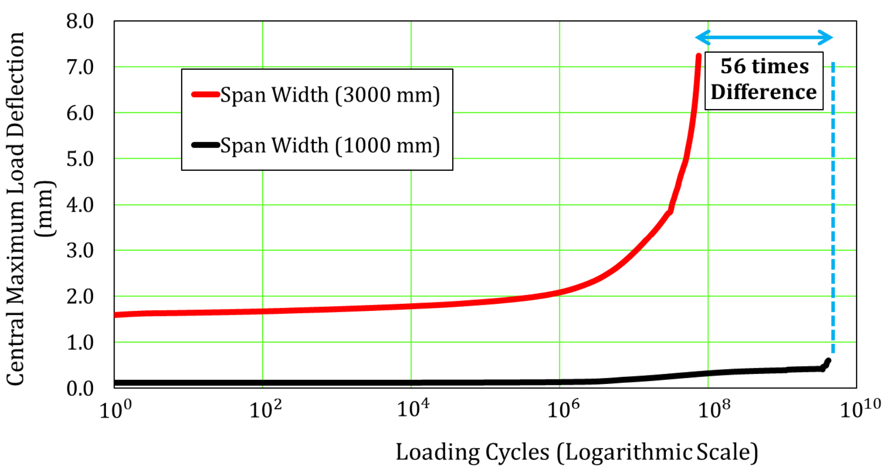

Fig. 15 Progression of central maximum load deflection with loading cycles for (1.0 and 3.0 meter) span-width cases.

ditions, it still takes time and pre-post effort. Every information such as drawings and material specifications is necessary before making FE mesh for the final check of performances. Step-by-step mesh generation and pre-post processing are also hard in many trial-and-error searching of probable dimensioning in addition to fatigue simulation. Then, FE simulation can be used to verify the structural performance at the final step or analyze new cases beyond the applicable range of experiences. On the other hand, as stated above, conceptual design is the process of deciding the shape and dimensioning of structures by repeating trial-and-error process to satisfy design requirements. It is difficult to conduct trial and error process with FE. Therefore, we need some supportive tool for this decision making process like ANN model.

Here, An ANN model is expected to be a tool to summarize and/or interpolate huge amount of FE-based computational results without burdens like mesh generation and computational time. There is an opinion that we still need empirical equations in design processes because AI models are not self-explanatory but a black box. It is generally hard to understand how an ANN model considers a specific problem by interpreting the weight matrices of the model. It just returns correct answer but it cannot show the physical meanings behind its calculations. Trial and error is not impossible to design structures with ANN model but it is still inefficient work for human. Visualization of way of thinking is necessary to utilize the knowledge of ANN for engineers. The authors think that the sensitivity analysis as shown in previous section can visualize inversely how the built ANN model behaves by monitoring change in life with the change of ANN's input variables. Empirical equations guided by sensitivity analysis are easier to understand for us by demonstrating the effectiveness of each parameter. As an empirical equation simplifies the complex results of the ANN model, both results have difference. Therefore, resultant design should be verified by ANN model at final step.

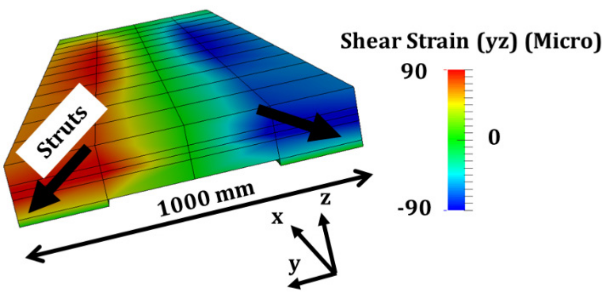


Fig. 16 Shear strain (yz) distribution among the transverse cross-section for the case of 1.0-meter span-width.

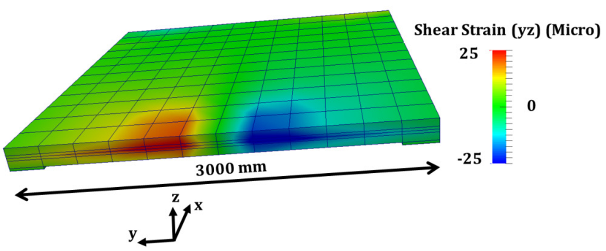


Fig. 17 Shear strain (yz) distribution among the transverse cross-section for the case of 3.0-meter span-width.

## 5.2 Empirical equation based on ANN model

Empirical equation (Equation 12) is proposed to estimate the fatigue life of RC decks guided by the findings of the sensitivity analysis of the introduced ANN model (Section 4.7). It should be noted that the proposed equation is obtained by fitting the results of the 75 samples that are used to build the ANN model, in addition to the knowledge achieved from the ANN sensitivity results.

**Figure 18** shows the accuracy of the proposed equation compared to multi-scale simulation for the 75 samples, where the regression coefficient (R) and the coefficient of variation (C.O.V) are 0.96 and 87%, respectively. These results demonstrate the reliability of the empirical equation regarding fatigue problems.

$$
\begin{aligned}
&\log(N) = -3.3 \times \log(P/Pv) + 6.5 \\
&Pv = (T^{2.66} \times e^{0.04 \times C} \times R^{0.2} \times W)/9600 \\
&W = 1.0 \quad \text{for S. T.} > 12.0 \\
&W = 1000 \times S.T.^{-2.87} \quad \text{for S. T.} \leq 12.0 \text{ (tied-arch action)}, \\
&\qquad\qquad T \leq 200 \text{ mm} \\
&W = 1000 \times S.T.^{-2.79} \quad \text{for S. T.} \leq 12.0 \text{ (tied-arch action)}, \\
&\qquad\qquad T > 200 \text{ mm} \\
&S.T. = S/T \quad \text{for } T \leq 200 \text{ mm (thin decks)} \\
&S.T. = S/T^{Z} \quad \text{for } T > 200 \text{ mm (thick decks)} \\
&Z = 0.07 \times \log(C) + 0.96 \quad \text{where } 1.04 \leq Z \leq 1.07
\end{aligned}
\tag{12}
$$

where, N is the number of cycles, P is the design wheel load (kN), $P_V$ is the virtual capacity of RC deck, T is the deck's thickness (mm), C is the compressive strength (MPa), R is the reinforcement ratio of transverse bottom rebar calculated from Equation 11, W is the effect of span-width in transverse direction, S is the span-width in the transverse direction (mm), S.T. is the effective span to thickness ratio, Z is a parameter considering the impact of compressive strength on the threshold of tied-arch mechanism. The virtual capacity $P_v$ used in this

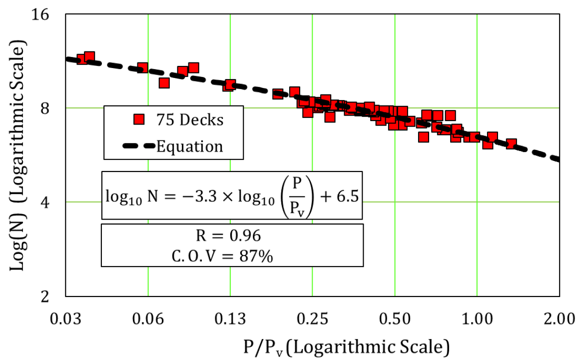


Fig. 18 Prediction of the proposed equation compared to multi-scale simulation.

Table 5 Properties of the analyzed decks from site (referred to in Fig. 4).

| No. | S(1) (mm) | T(2) (mm) | C(4) (MPa) | TB-D(7) (mm) | TB-S(8) (mm) |
|---|---|---|---|---|---|
| 1 | 3400 | 180 | 24 | 16 | 100 |
| 2 | 2400 | 170 | 24 | 16 | 100 |
| 3 | 3500 | 180 | 30 | 16 | 100 |
| 4 | 2800 | 200 | 24 | 16 | 100 |
| 5 | 3100 | 190 | 24 | 16 | 100 |
| 6 | 2900 | 220 | 35 | 22 | 150 |
| 7 | 2200 | 210 | 35 | 16 | 100 |
| 8 | 3500 | 210 | 35 | 16 | 100 |
| 9 | 2300 | 160 | 24 | 16 | 100 |
| 10 | 2850 | 210 | 35 | 19 | 150 |
| 11 | 2600 | 230 | 24 | 19 | 125 |
| 12 | 2800 | 230 | 24 | 19 | 125 |
| 13 | 2500 | 200 | 24 | 19 | 125 |
| 14 | 2600 | 210 | 24 | 19 | 125 |

equation is different from the static strength because failure mode in high cycle wheel-type loads is different from the static punching shear failure. Therefore, the base strength is not necessarily the static strength.

### 5.3 Comparison of empirical equation and ANN model

The empirical equation is compared with the ANN model, by preparing a new dataset of in-service RC decks from sites in Japan. **Table 5** shows the dimensions, rebar, and material properties for a total number of 14 decks. **Figure 19** shows the comparison of the fatigue life prediction of Equation 12 and the ANN model for the analyzed decks, where the coefficient of variation (C.O.V) of prediction is 83%. In practice, S-N diagrams of fatigue life allow a range of ±(10~13)% difference in stress levels which is in the range of the factor of safety utilized in the engineering practice (JSCE 2007). This magnitude of stress drift corresponds to ±(200~300)% difference in the fatigue life on the logarithmic scale. In most cases, the difference of empirical equation from ANN model is within the allowable range. The difference is relatively high in case of

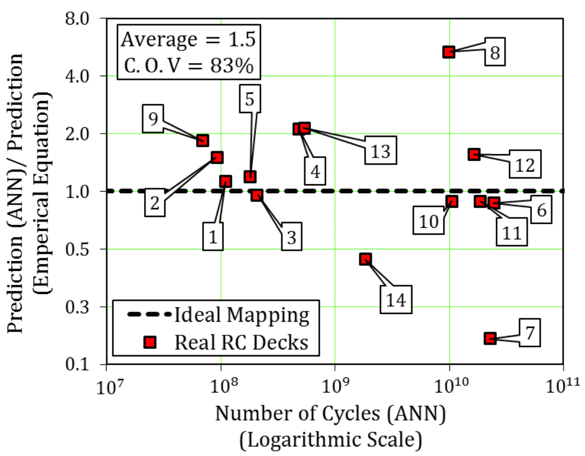


Fig. 19 Empirical formula and ANN model with properties of real RC decks.

the high compressive strength with small reinforcement ratios. If several parameters change simultaneously away from the referential case, the difference between ANN model and the empirical equation tends to be significant. Even though, the difference remains within one order even in the rest cases. Then, the empirical equation is useful enough to decide properties of materials and dimensions of structural members. As stated before, a final check is needed because the empirical equation of simplified functions is just the interpolation of the past experiences.

## 6. Conclusions

In this research, fatigue failure of RC deck under moving wheel load is directly simulated by validated multiscale analysis. Then, ANN model is strictly built for the fatigue life perdition of newly constructed RC decks based upon various RC decks with wide range of properties. The proposed model is discussed in terms of conceptual design of RC deck. Finally, an empirical equation is introduced and has been compared with the proposed ANN model for real RC decks from site. Based on the proposed models and simulation results, the following conclusions are drawn.

(1) ANN model, which is made from computational results of multi-scale analysis with wide range of RC decks, covers various failure modes such as punching shear and crushing of tied-arch. Empirical equation achieved by sensitivity analysis of ANN model also includes various failure modes while past empirical equation assumed only punching shear mode.
(2) The proposed ANN model offers to predict the fatigue life of newly constructed RC deck in just seconds without the need of running complex simulation programs.
(3) The generalization of the proposed ANN model is secured by conducting leave-one-out cross-validation and testing among unknown data.
(4) Assessment procedure of the impact of deck's properties on fatigue life is proposed with regard to ANN model. Achieved sensitivities are useful to construct the conceptual design of RC decks.
(5) It is found that the ANN model captures tied-arch action of RC decks that lead to extend the fatigue life significantly.
(6) The empirical equation guided by ANN model enables to conduct preliminary design of RC decks. On the other hand, final check by ANN model ensures the performance of designed RC decks.


## Acknowledgment

This study was financially supported by Council for Science, Technology, and Innovation, "Cross-ministerial Strategic Innovation Promotion Program (SIP), Infrastructure Maintenance, Renovation, and Management" granted by JST.

## References

Bakht, B., (1996). "Revisiting arching in deck slabs." *Canadian Journal of Civil Engineering*, 23(4), 973-981.

Burden, F. and Winkler, D., (2008). "*Bayesian regularization of neural networks.*" Artificial Neural Networks. Humana Press.

Cady, P. D. and Weyers, R. E., (1983). "Chloride penetration and the deterioration of concrete bridge decks." *Cem. Concr. Aggreg.*, 5, 81-87.

CSA, (2014). "*Canadian highway bridge design code*." Mississauga: Canadian Standards Association.

Detwiler, R. J., Kojundic, T. and Fidjestol, P., (1997). "Evaluation of bridge deck overlays." *Concr. Int. Detroit*, 19(8), 43-46.

Fathalla, E., Tanaka, Y. and Maekawa, K., (2018a). "Remaining fatigue life assessment of in-service road bridge decks based upon artificial neural networks." *Engineering Structures*, 171, 602-616.

Fathalla, E., Tanaka, Y. and Maekawa, K., (2018b). "Quantitative deterioration assessment of road bridge decks based on site inspected cracks." *Applied Sciences*, 8, 1197.

Fathalla, E., Tanaka, Y. and Maekawa, K., (2018c). "Fatigue life estimation of road bridge decks by utilizing multi-scale simulation and artificial intelligence." In: *Proceedings of the 4th International Conference on Service Life Design for Infrastructures (SLD4)*, Delft, Netherlands, PRO 125.

Fathalla, E., Tanaka, Y., Maekawa, K. and Sakurai, A., (2019a). "Quantitative deterioration assessment of road bridge decks based on site inspected cracks under stagnant water." *J. Adv. Concr. Technol.*, 17(1), 16-33.

Fathalla, E., Tanaka, Y. and Maekawa, K., (2019b). "Fatigue life of RC bridge decks affected by non-uniformly dispersed stagnant water." *Appl. Sci.*, 9(3), 607.

Fathalla, E., Tanaka, Y. and Maekawa, K., (2019c). "Effect of crack orientation on fatigue life of reinforced concrete bridge decks." *Appl. Sci.*, 9(8), 1644.

Fausett, L. V., (1994). "*Fundamentals of neural networks: architectures, algorithms, and applications*." Englewood Cliffs: Prentice-Hall.

Fenwick, R. C. and Thomas P., (1968). "Mechanism of shear resistance of concrete beams." *Journal of the Structural Division*, 94(10), 2325-2350.

*fib*, (2006). "Model code for service life design." Bulletin No. 34, In: J. Walraven, Ed. *fib Model Code for Concrete Structures 2010*, Hoboken New Jersey: Ernst & Sohn.

Foresee, F. D. and Hagan, M., (1997). "Gauss-newton approximation to Bayesian regularization." *Proceedings of International Joint Conference on Neural Networks.*

Freyermuth, C. L., Klieger, P., Stark, D. C. and Wenke, H. N., (1970). "Durability of concrete bridge decks—A review of cooperative studies." *Highw. Res. Rec.*, 328, 50-60.

Fujiyama, C., Tang, X. J., Maekawa, K. and An, X., (2013). "Pseudo-cracking approach to fatigue life assessment of RC bridge decks in service." *J. Adv. Concr. Technol.*, 11(1), 7-21.

Fujiyama, C., Matsumura, T. and Takasuka, T., (2014). "Failure process of steel-concrete composite bridge deck subjected to repetition of moving load in three dimensional non-linear FE analysis." *Journal of Japan Society of Civil Engineers*, A1, 70(2), 227-237.

Geisser, S., (1993). "*Predictive inference.*" New York: Chapman and Hall.

Grossberg, S., (1982). "*Studies of the mind and brain.*" Drodrecht, Holland: Reidel Press.

Hagan, M. T. and Menhaj, M., (1994). "Training feed-forward networks with the Marquardt algorithm." *IEEE Transactions on Neural Networks*, 15(6), 989-993.

Hagan, M. T., Demuth, H. B., Beale, M. H. and Jesús, O. D., (1996). "*Neural network design.*" Boston: PWS Publishing.

Hiratsuka, Y., Senda, M., Fujiyama, C. and Maekawa, K., (2016). "Fatigue based structural behavior of RC bridge slabs with different loading histories." *Journal of Japan Society of Civil Engineers*, E2, 72(4), 323-342.

Isobe, R., Tsuno, K., Iwaki, I., Kishi, T. and Nakazawa, J., (2015). "Study on the fatigue durability of the RC road bridge deck combined with lightweight aggregate and expansive additive." *Journal of JSCE E2*, 71(2), 191-202.

JRA, (2012). "*Specification for highway bridges-part III Concrete bridges*." Tokyo, Japan: Japan Road Association.

JSCE, (2007). "*Standard specification for concrete structures (design)*." Tokyo, Japan.

Kim, D., Kim, W. and White, R. N., (1999). "Arch action in reinforced concrete beams—A rational prediction of shear strength." *Structural Journal*, 96(4), 586-593.

Lee, M. K. and Barr, B. I. G., (2004). "An overview of the fatigue behaviour of plain and fibre reinforced concrete." *Cement and Concrete Composites*, 26(4), 299-305.

Lindquist, W. D., Darwin, D., Browning, J. and Miller, G. G., (2006). "Effect of cracking on chloride content in concrete bridge decks." *ACI Material Journal*, 103(6), 467-473.

M. I. T Lincoln Laboratory, (1989). "*DARPA neural network study*." Defense Technical Information Center.

MacKay, D. J., (1992). "Bayesian interpolation." *Neural Computation*, 4(3), 415-447.

Maekawa, K. and Fujiyama, C., (2013a). "Crack water interaction and fatigue life assessment of RC bridge decks." *Poromechanics V: ASCE*, 2280-2289.

Maekawa, K. and Fujiyama, C., (2013b). "Rate-dependent model of structural concrete incorporating kinematics of ambient water subjected to high-cycle load."

*Engineering Computations*, 30(6), 825-841.
Maekawa, K., Ishida, T. and Kishi, T., (2009). "*Multi-scale modeling of structural concrete.*" London: Taylor & Francis.
Maekawa, K., Ishida, T., Chijiwa, N. and Fujiyama, C., (2015). "Multiscale coupled-hygromechanistic approach to the life-cycle performance assessment of structural concrete." *ASCE, Journal of Materials in Civil Engineering*, 27(2), A4014003.
Maekawa, K., Pimanmas, A. and Okamura, H., (2003). "*Nonlinear mechanics of reinforced concrete.*" London: Spon Press.
Maekawa, K., Toongoenthong, K., Gebreyouhannes, E. and Kishi, T., (2006a). "Direct path-integral scheme for fatigue simulation of reinforced concrete in shear." *Journal of Advanced Concrete Technology*, 4(1), 159-177.
Maekawa, K., Gebreyouhannes, E., Mishima, T. and An, X., (2006b). "Three-dimensional fatigue simulation of RC slabs under traveling wheel-type loads." *Journal of Advanced Concrete Technology*, 4(3), 445-457.
Maeshima, T., Koda, Y., Tsuchiya, S. and Iwaki, I., (2014). "Influence of corrosion of rebars caused by chloride induced deterioration on fatigue resistance in RC road deck." *Journal of Japan Society of Civil Engineers*, E2, 70(2), 208-225
Matsui, S., (1987). "Fatigue strength of RC-slabs of highway bridge by wheel running machine and influence of water on fatigue." *Proc. of JCI*, 9(2), 627-632.
Matsui, S., (2007). "*Bridge decks of highway, design, construction and maintenance*." Tokyo: Morikita Publishing. (in Japanese)
Matsui, S. and Maeda, Y., (1986). "A rational evaluation method for deterioration of highway bridge decks." *Journal of Japan Society of Civil Engineers*, 374, 419-426.
Murphy, K. P., (2012). "*Machine learning: A probabilistic perspective.*" Cambridge, Massachusetts: The MIT Press.
Ohta, K., Tanikura, I., Tachibana, Y., Shionaga, R., Okubo, F. and Kajio, S., (2015). "Studies of damages of concrete bridge decks in America." *Bridge and Foundation Engineering*, 9, 33-39.
Okada, K., Okamura, H., Sonoda, K. and Shimada, I., (1982). "Cracking and fatigue behavior of bridge deck RC slabs." *Journal of JSCE*, 321, 49-61.
Picard, R. R. and Cook, R. D., (1984). "Cross-validation of regression models." *Journal of the American Statistical Association*, 79, 575-583.
Rankin, G. I. B. and Long, A. E., (1997). "Arching action strength enhancement in laterally-restrained slab strips." *Proceedings of the Institution of Civil Engineers-Structures and Buildings,* 122(4), 461-467.
Rumelhart, D., Hinton, G. and Williams, R., (1986). "Learning representations by back-propagating errors." *Nature*, 323, 533-536.
Sakulich, A. R. and Bentz, D. P., (2011). "Increasing the service life of bridge decks by incorporating phase-change materials to reduce freeze-thaw cycles." *J. Mater. Civ. Eng.*, 24(8), 1034-1042.
Schläfli, M. and Brühwiler, E., (1998). "Fatigue of existing reinforced concrete bridge deck slabs." *Engineering Structures*, 20(11), 991-998.
Shah, S. P., Weiss, W. J. and Yang, W., (1998). "Shrinkage cracking—Can it be prevented?" *Concr. Int.*, 20(4), 51-55.
Sparks, P. R. and Menzies, J. B., (1973). "The effect of rate of loading upon the static and fatigue strengths of plain concrete in compression." *Magazine of Concrete Research*, 25(83), 73-80.
Tanaka, Y., Maekawa, K., Maeshima, T., Iwaki, I., Nishida, T. and Shiotani, T., (2017). "Data assimilation for fatigue life assessment of RC bridge decks coupled with hygro-mechanistic model and nondestructive inspection." *Journal of Disaster Research*, 12(3), 422-431.
Tepfers, R. and Kutti, T., (1979). "Fatigue strength of plain, ordinary, and lightweight concrete." *ACI Journal*, 76(5), 635-652.
Ulm, F. J., Coussy, O., Kefei, L. and Larive, C., (2000). "Thermo-chemo-mechanics of ASR expansion in concrete structures." *J. Eng. Mech.*, 126(3), 233-242.
Val, D. V., Stewart, M. G. and Melchers, R. E., (1998). "Effect of reinforcement corrosion on reliability of highway bridges." *Eng. Struct.*, 20(11), 1010-1019.
Vassie, P., (1984). "Reinforcement corrosion and the durability of concrete bridges." In: *Proceedings of Institution of Civil Engineers; Institution of Civil Engineers*: London, UK, 76(1), 713-723.
Waagaard, K., (1982). "Fatigue strength evaluation of offshore concrete structures." *ACI*-SP-75, 373-397.
Walraven, J., (editor) (2013). "*fib model code for concrete structures 2010*." Hoboken New Jersey: Ernst & Sohn.
Zararis, P. D. and Papadakis, G. C., (2001). "Diagonal shear failure and size effect in RC beams without web reinforcement." *Journal of Structural Engineering*, 127(7), 733-742.